



Transition of Dephospho-DctD to the Transcriptionally Active State via Interaction with Dephospho-IIA^{Glc}

Sebin Kang,^a  Kyu-Ho Lee^a

^aDepartment of Life Science, Sogang University, Seoul, South Korea

ABSTRACT Exopolysaccharides (EPSs), biofilm-maturing components of *Vibrio vulnificus*, are abundantly produced when the expression of two major EPS gene clusters is activated by an enhancer-binding transcription factor, DctD₂, whose expression and phosphorylation are induced by dicarboxylic acids. Surprisingly, when glucose was supplied to *V. vulnificus*, similar levels of expression of these clusters occurred, even in the absence of dicarboxylic acids. This glucose-dependent activation was also mediated by DctD₂, whose expression was sequentially activated by the transcription regulator NtrC. Most DctD₂ in cells grown without dicarboxylic acids was present in a dephosphorylated state, known as the transcriptionally inactive form. However, in the presence of glucose, a dephosphorylated component of the glucose-specific phosphotransferase system, d-IIA^{Glc}, interacted with dephosphorylated DctD₂ (d-DctD₂). While d-DctD₂ did not show any affinity to a DNA fragment containing the DctD-binding sequences, the complex of d-DctD₂ and d-IIA^{Glc} exhibited specific and efficient DNA binding, similar to the phosphorylated DctD₂. The d-DctD₂-mediated activation of the EPS gene clusters' expression was not fully achieved in cells grown with mannose. Furthermore, the degrees of expression of the clusters under glycerol were less than those under mannose. This was caused by an antagonistic and competitive effect of GlpK, whose expression was increased by glycerol, in forming a complex with d-DctD₂ by d-IIA^{Glc}. The data demonstrate a novel regulatory pathway for *V. vulnificus* EPS biosynthesis and biofilm maturation in the presence of glucose, which is mediated by d-DctD₂ through its transition to the transcriptionally active state by interacting with available d-IIA^{Glc}.

IMPORTANCE Transcription regulation by bacterial two-component systems is achieved by a response regulator upon its transition to the transcriptionally active form via kinase activity of its cognate sensor under specific conditions. A well-known response regulator, DctD, is converted to its phosphorylated form when DctB senses ambient dicarboxylic acids. Phospho-DctD induces expression of its regulon, including the gene clusters for biosynthesis of exopolysaccharides (EPSs), the essential constituents of biofilm matrix. In the absence of dicarboxylic acids, however, DctD-mediated induction of these EPS gene clusters and biofilm maturation was observed if glucose was supplied. This suggests that dephospho-DctD could play a role in activating the transcription of target genes. A component of glucose-phosphotransferase system, IIA^{Glc}, was present in a dephosphorylated state in the presence of glucose. Dephospho-DctD formed a complex with dephospho-IIA^{Glc} and was converted to a transcriptionally active state. These findings suggest the other response regulators could also have alternative pathways of activation independent of phosphorylation.

KEYWORDS biofilm, dephospho-DctD, dephospho-IIA^{Glc}, exopolysaccharides, glucose

A major bacterial regulatory system in response to fluctuating environmental parameters is the two-component system (TCS), in which the sensor, a histidine protein kinase, transduces environmental signals to its cognate response regulator (1, 2). Most bacteria have numerous TCSs that control a wide range of cellular responses by

Editor Matthew Parsek, University of Washington

Copyright © 2022 Kang and Lee. This is an open-access article distributed under the terms of the [Creative Commons Attribution 4.0 International license](https://creativecommons.org/licenses/by/4.0/).

Address correspondence to Kyu-Ho Lee, kyuholee@sogang.ac.kr.

The authors declare no conflict of interest.

Received 26 December 2021

Accepted 22 February 2022

Published 21 March 2022

regulating the expression or activity of their specific regulons via the transition of the response regulators between inactive and active states (3). The alteration of a response regulator to the active state is initiated once its cognate sensor kinase is autophosphorylated at a histidine residue upon exposure to specific environmental signals, such as various kinds of carbon, nitrogen, phosphorus, or sulfur sources (4–6). Phosphotransfer then rapidly occurs from the histidine residue in a sensor kinase to the aspartic acid residue in a response regulator. Phosphorylation usually induces a conformational change in response regulators, which endows the inactive regulators with the ability to perform specific outputs: for example, binding to the corresponding targets of DNA, RNA, or proteins (7, 8).

More than 65% of the so-far-identified response regulators are transcription factors that exhibit DNA-binding affinity if phosphorylated. Approximately 15% of them are categorized into the bacterial enhancer binding protein (bEBP) family, which is further subdivided into five groups based upon the structural characteristics in their N-terminal regulatory domains (9–13). In group I of bEBPs, which includes the well-known NtrC family, the transcriptionally active forms are phosphorylated oligomers, such as hexamers or heptamers. Regardless of the phosphorylation state of the monomeric form, the dimeric forms of bEBP are formed. However, further assembly to the oligomeric forms requires phosphorylation of the dimers, by which the AAA⁺ ATPase motifs located in the central domain of bEBP are conformationally opened to hydrolyze ATP. The produced hexamers or heptamers are then capable of binding to the upstream activator sequences for the target genes and interact with RpoN in the promoters via involvement of the C-terminal DNA-binding domain and the GAFTGA loop in the central domain of bEBP, respectively. ATP hydrolysis is necessary for the oligomeric forms of bEBP to initiate the transcription process by stabilizing these interactions (12).

DctD, belonging to group I bEBPs, has been extensively studied in nitrogen-fixing bacteria, in which the dicarboxylic acids transported from the host's roots are the main sources of electrons, reducing dinitrogen to ammonia (14). Its sensor kinase, DctB, senses the ambient dicarboxylic acids and phosphorylates DctD, which in turn activates the transcription of genes encoding the uptake system(s) for dicarboxylic acids (15). In addition to nitrogen-fixing bacteria, many bacterial species, including the model foodborne pathogen *Vibrio vulnificus*, are also equipped with DctBD (16). In the genomes of *V. vulnificus*, two operons encoding the DctBD homologs, *dctB₁D₁* and *dctB₂D₂*, are present, but it was found that DctD₂ is responsible for activating the transcription of exopolysaccharide (EPS) EPS-II and EPS-III clusters in the presence of fumarate (16). Notably, biosynthesis of EPSs, the loosely associated polysaccharides outside bacterial envelopes (17), is regulated at the transcription level via the involvement of DctD₂, which activates the expression of EPS gene clusters in the presence of various kinds of dicarboxylic acids (16). Furthermore, the transcription of the *dctB₂D₂* operon is activated by NtrB/C, the TCS responsive to the carbon/nitrogen ratio (16). The findings that the production and secretion of EPSs, which are presumed to be entirely composed of carbohydrates, are regulated by both NtrB/C and DctB₂/D₂ have implied the presence of a common regulatory connection or connections in bacterial recognition of the depletion of nitrogen sources and the repletion of some carbon sources.

A dramatic example of bacterial adaptational behavior at the population level is the formation of biofilms in response to various environmental conditions, which enhances the survival of individual cells under stress conditions, including the host environment (18, 19). EPSs are the most abundant constituents comprising the extracellular polymeric matrix (EPM) of biofilms and the highly active components interacting with other EPM components: e.g., proteins, polysaccharides, nucleic acids, and lipids (17, 20–25). Thus, EPSs are considered essential constituents for the construction of mature biofilms by facilitating the interactions of a bacterial cell with adjacent cells and substrates (26). *V. vulnificus* has a high risk of causing fatal septicemia or gastroenteritis (27); it has been shown that its ability to form mature biofilms is critically dependent upon the biosynthesis of EPSs (28). There are at least three gene clusters in *V. vulnificus* genomes: EPS-I (the *rbd* operon), EPS-II (the *brp* operon), and EPS-III (28–30). The EPS-II and EPS-III

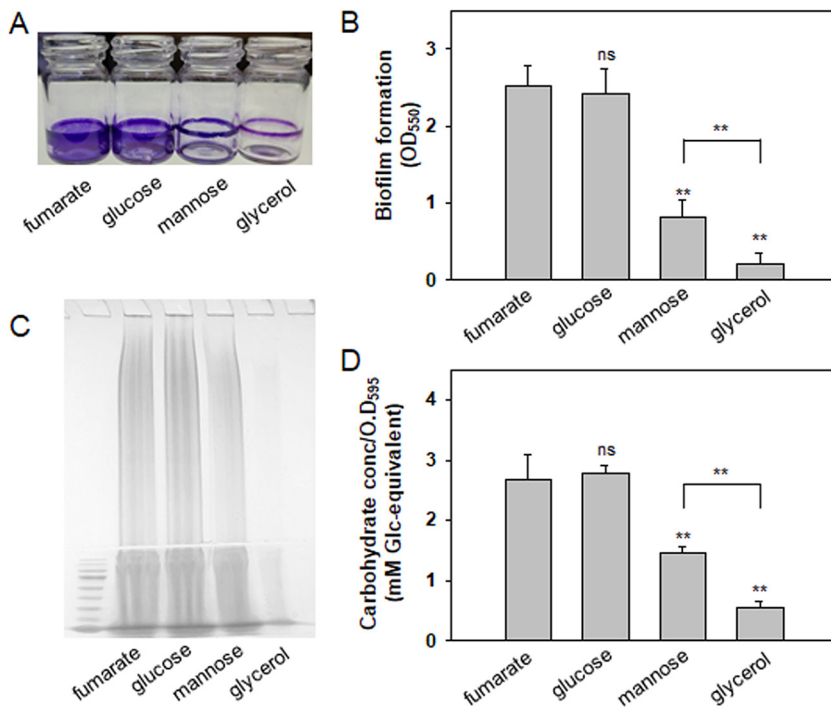


FIG 1 Biofilm formation and EPS production by *V. vulnificus* in the presence of fumarate, glucose, mannose, or glycerol. (A and B) Biofilm formation. Wild-type *V. vulnificus* cells were statically incubated for 48 h in AB medium supplemented with fumarate, glucose, mannose, or glycerol. The biofilms that developed on the borosilicate tubes were estimated by staining with crystal violet (A). The associated dyes were dissolved and measured by spectrophotometry at 550 nm (B). The *P* values for comparison with the AB-fumarate incubation are indicated (**, $P < 0.001$; *, $0.001 \leq P < 0.01$; ns, not significant). A comparison between AB-mannose and AB-glycerol incubations was also included with a *P* value above a corresponding horizontal line. (C and D) EPS production. Wild-type *V. vulnificus* cells grown on the AB agar plates supplemented with fumarate, glucose, mannose, or glycerol, were subjected to the process for EPS extraction, as previously described (28). The resultant EPS extracts run in a 5% stacking polyacrylamide gel were visualized by staining with Stains-All (C). The carbohydrate contents in each extract were measured by the phenol-sulfuric acid method (64). The estimated carbohydrate contents were expressed as mM glucose equivalents per cell masses equivalent to an OD₅₉₅ of 1.0 (D). *P* values are presented as described above.

clusters are required for production of EPSs involved in biofilm maturation under the conditions containing dicarboxylic acids, although EPS compositions have not yet been elucidated in this bacterial species (28, 31). One of the major regulators for induction of these clusters has been shown to be DctB/D (16).

The abilities of *V. vulnificus* to form mature biofilms and to disperse cells from the robust biofilm structures have been correlated with its pathogenicity in an animal model (28, 31, 32). As shown in diverse pathogenic bacteria (33, 34), it is assumed that the assembly of biofilms and the dispersal from these structures would provide *V. vulnificus* with the advantages of survival and proliferation in host environments. Therefore, appropriate expression of EPS gene clusters is required for this foodborne pathogen upon its sensing host-specific environments, such as carbon sources that are relatively abundant in host environments. Among the various available carbon sources, glucose is abundantly present in various biofluids, tissues, and organs of humans (35, 36), and its uptake and utilization are controlled by the phosphotransferase system (PTS) and diverse regulatory mechanisms, including carbon catabolite repression (37, 38).

In our preliminary investigation to screen the factors inducing biofilm formation of *V. vulnificus*, it was noticed that glucose was able to induce biofilm maturation via increasing the biosynthesis of EPSs by virtue of the transcription factor DctD₂ (shown in Fig. 1), similar to dicarboxylic acids. Interestingly, DctD₂ is presumed to be present in an unphosphorylated, inactive form in the absence of dicarboxylic acids. Thus, in this

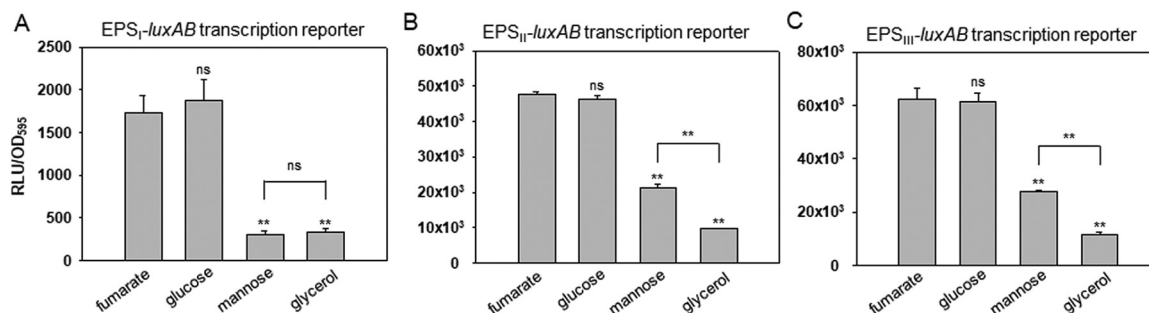


FIG 2 Expression of three EPS gene clusters of *V. vulnificus* in the presence of fumarate, glucose, mannose, or glycerol. Wild-type *V. vulnificus* cells carrying a *luxAB* transcriptional reporter fused with each EPS gene cluster (EPS-I [A], EPS-II [B], or EPS-III [C]) (28) were grown in AB-fumarate, -glucose, -mannose, or -glycerol medium supplemented with 3 μ g/mL tetracycline. At an OD₅₉₅ of 0.4, cells were harvested, and their luciferase activities were measured using a luminometer. The degree of cluster expression was expressed as a normalized value: the relative light unit (RLU) divided by the cell mass (OD₅₉₅) of each sample. The *P* values are presented as described in the legend to Fig. 1.

study, we further investigated the regulatory mechanism that activates the expression of EPS gene clusters in the presence of glucose, which mimics the regulatory role of the phosphorylated form of DctD₂.

RESULTS

Biofilm formation and EPS production by *V. vulnificus* were highly induced in the presence of glucose. It has been previously shown that *V. vulnificus* produces significantly increased sizes of biofilms under growth conditions supplemented with dicarboxylic acids, such as fumarate, compared to biofilms formed in the presence of glycerol (16). In this study, to further examine the effects of other carbon sources on biofilm formation by *V. vulnificus*, the wild-type (WT) strain of this bacterium was incubated for 48 h in AB medium (defined in Materials and Methods) containing PTS sugars, such as glucose and mannose. The resultant biofilms were compared with those formed in AB-fumarate or AB-glycerol (Fig. 1A). In the presence of glucose, the extent of biofilm formation was almost the same as that in the presence of fumarate. In contrast, biofilms formed in AB-mannose were intermediate between those in AB-fumarate and AB-glycerol (Fig. 1B): The biofilms formed in AB-mannose were estimated to be 0.3 \times and 3.8 \times the sizes of the biofilms formed in AB-fumarate and AB-glycerol, respectively.

The differences in biofilm formation were well correlated with the degree of EPS production by *V. vulnificus* cells in the presence of the same kinds of carbon sources supplied in the AB medium (Fig. 1C). The levels of EPS production by wild-type *V. vulnificus* cells grown in the presence of glucose were 1.0, 1.9, and 5.1 times higher than those by the cells grown in the presence of fumarate, mannose, and glycerol, respectively (Fig. 1D). These results imply that the biosynthetic factors for EPSs, the most critical components for biofilm maturation by *V. vulnificus*, were similarly expressed in *V. vulnificus* grown in the presence of fumarate or glucose.

Increased production of EPS in the presence of glucose was due to the induced expression of EPS-II and EPS-III gene clusters. Since EPS production is regulated at the transcriptional levels of three gene clusters for EPS biosynthesis in *V. vulnificus* (28), the effects of glucose and mannose on the expression of the EPS gene clusters were examined using *V. vulnificus* carrying a *luxAB* transcription reporter fused with the upstream region of each EPS cluster. All three EPS clusters were highly induced in AB-fumarate compared to AB-glycerol, as previously shown (16, 28). The clusters were also well expressed in AB-glucose, with almost the same degree of expression in AB-fumarate (Fig. 2A to C). In AB-mannose, the expression of the EPS-I cluster, which is directly activated by NtrC (16), was significantly decreased to basal levels, as shown in AB-glycerol (Fig. 2A). However, the levels of expression of EPS-II and EPS-III clusters in AB-mannose, which are directly activated by DctD₂ (16), were significantly lower than those in AB-glucose, but higher than those in AB-glycerol (Fig. 2B and C). These results suggest

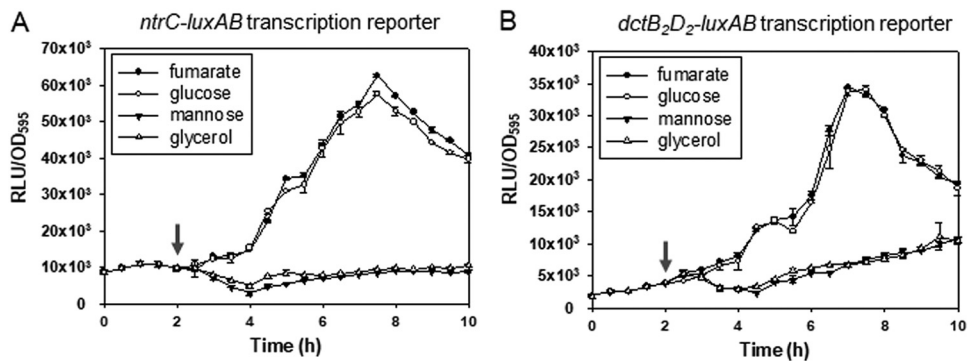


FIG 3 Expression of *ntrC* and *dctD₂* genes of *V. vulnificus* in the presence of fumarate, glucose, mannose, or glycerol. Wild-type *V. vulnificus* cells carrying a *luxAB* transcriptional reporter fused with the regulatory region of the *glnA-ntrB-ntrC* operon (32) (A) or the regulatory region of the *dctB₂D₂* operon (16) (B) were grown for 2 h in AB medium supplemented with glycerol (22 mM) and tetracycline (3 μ g/mL) and then subcultured to AB-fumarate, -glucose, -mannose, and -glycerol media supplemented with 3 μ g/mL tetracycline. Bacterial cells were harvested at every 30 min, and light production was measured and presented as described in the legend to Fig. 2. The arrows indicate the point at which *V. vulnificus* cells pregrown in AB-glycerol were challenged with different carbon sources.

that the significantly increased levels of biofilm formation and EPS production in AB-glucose (Fig. 1), compared to those in AB-mannose, were due to the increased transcription levels of the EPS gene clusters, possibly via the involvement of DctD even in the presence of glucose.

As previously reported (16), among two DctD homologs in *V. vulnificus*, only DctD₂ has an amino acid residue (D57) that can be phosphorylated in the presence of dicarboxylic acids. Thus, DctD₂ is a transcription factor responsible for activating the transcription of EPS-II and EPS-III clusters in the presence of fumarate (16). Since DctD cannot be phosphorylated without a dicarboxylic acid, the dephosphorylated forms of DctD, which could be either a dephosphorylated DctD₂ or a naturally unphosphorylated DctD₁, would activate the transcription of the clusters. Thus, to identify the functional DctD(s) in transcriptional activation of the gene clusters in the presence of glucose, *V. vulnificus* strains carrying *luxAB* transcription reporter fused with *dctA*, one of the representative genes belonging to the DctD regulon (15, 16), were grown in AB medium containing fumarate, glucose, mannose, or glycerol (see Fig. S1 in the supplemental material). Its expression in the Δ *dctD₁* mutant was similar to that in the wild type. Furthermore, its expression patterns were similar to those of EPS-II and EPS-III clusters in the wild type: expression was high in AB-fumarate and AB-glucose, intermediate in AB-mannose, and basal in AB-glycerol. However, expression of *dctA* in the Δ *dctD₂* mutant was minimal regardless of the carbon source in the growth medium, demonstrating that DctD₂ is required for induction of the transcription of *dctA*.

Both *ntrC* expression and *dctD* expression were induced by glucose. Since the maximal degrees of expression of the EPS-II and EPS-III clusters were observed in cells grown in the presence of fumarate or glucose (Fig. 2), the expression of DctD₂ was examined by measuring the transcription of the genes encoding DctD₂ as well as its transcription activator, NtrC. As it was previously reported that *ntrC* transcription was induced in the presence of dicarboxylic acids and then NtrC activated the *dctD₂* transcription (16), whether glucose exhibited a similar effect on the expression of NtrC and DctD₂ was investigated (Fig. 3). *V. vulnificus* carrying *luxAB* transcription reporters fused with DNA fragments upstream of the *glnA-ntrB-ntrC* operon or the *dctB₂D₂* operon were grown in AB-glycerol. After 2 h of incubation, fumarate, glucose, mannose, or glycerol was added to each culture. The basal levels of the *ntr*-reporter (Fig. 3A) and *dct₂*-reporter (Fig. 3B) fusions in AB-glycerol for the first 2 h of incubation were highly induced by the addition of fumarate and glucose. In contrast, the addition of mannose did not result in the induction of either reporter, as shown by glycerol. These results

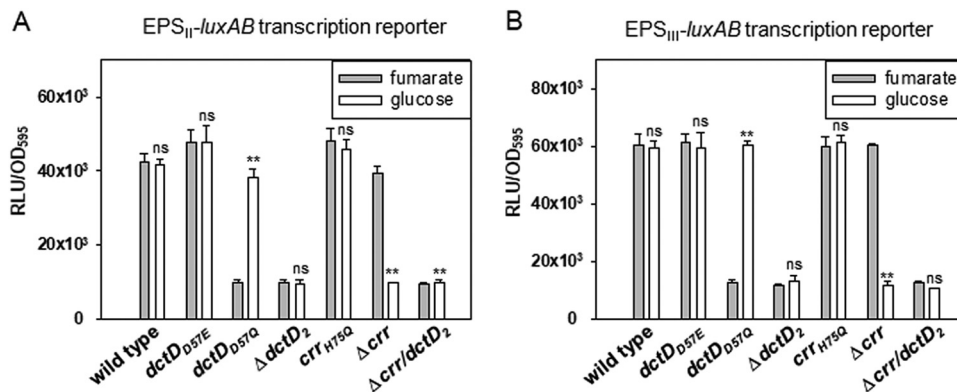


FIG 4 Expression of the EPS-II and EPS-III gene clusters in various mutant *V. vulnificus* strains defective in DctD₂ and/or IIA^{Glc}. *V. vulnificus* strains carrying mutant DctD₂ (i.e., ΔdctD₂, a phospho-form of DctD [*dctD*_{D57E}], and a dephospho-form of DctD [*dctD*_{D57Q}]), mutant IIA^{Glc} (i.e., Δcrr and a dephospho-form of IIA^{Glc} [*crr*_{H75Q}]), or deletion of two ORFs (Δcrr ΔdctD₂) were used to compare the expression of two EPS gene clusters. Each strain carrying either EPS-II (A) or EPS-III (B) was inoculated in AB-fumarate and AB-glucose media. After incubation for 4 h, the cell densities and light production were measured, and the extents of the gene clusters' expression were presented as described in the legend to Fig. 2. The *P* values for comparison with the samples in fumarate and glucose are indicated: **, *P* < 0.001; ns, not significant.

showed that glucose induces the expression of both *ntrC* and *dctD₂*. Since NtrC activates the transcription of *dctB₂D₂* operon, as previously reported (16), it is postulated that the induced NtrC activated *dctD₂* transcription, and then the increased expression of DctD₂ would subsequently result in the induced expression of EPS-II and EPS-III clusters in AB-glucose.

The dephosphorylated form of DctD₂ activated the transcription of the EPS-II and EPS-III gene clusters in the presence of the dephosphorylated form of IIA^{Glc}.

Transcriptional activation of the EPS-II and EPS-III clusters occurs via phosphorylation of DctD₂ by dicarboxylic acids, specifically fumarate (16). Thus, it is questionable how dephosphorylated DctD₂ (d-DctD₂) in cells grown in the presence of glucose could play a role in activating transcription as phosphorylated DctD₂ (p-DctD₂) in cells grown with fumarate. To address this issue, various strains of *V. vulnificus* mutated at the *dctD₂* locus were utilized to monitor the expression of two *luxAB*-reporters. This experiment included the strains in which *dctD₂* was deleted (ΔdctD₂), substituted for with an open reading frame (ORF) encoding p-DctD₂ (*dctD*_{D57E}), and substituted for with an ORF encoding d-DctD₂ (*dctD*_{D57Q}). Each strain carrying a reporter of either EPS-II (Fig. 4A) or EPS-III (Fig. 4B) was inoculated in AB-fumarate and AB-glucose media, and their expression at the mid-exponential phase was determined. Basal levels of expression occurred in the ΔdctD₂ mutant, which further supported the dependency of two clusters' transcriptions on DctD₂ under both incubation conditions. In the *dctD*_{D57E} strain, the expression of two clusters in either AB-fumarate or AB-glucose was at maximal levels, which was achieved by p-DctD₂ regardless of the carbon sources in the growth medium. The expression of two reporters in the *dctD*_{D57Q} strain, however, was induced only in AB-glucose up to the expression levels in the *dctD*_{D57E} strain, suggesting that d-DctD₂ plays a critical role in activating the clusters' transcription in AB-glucose. The findings indicated that the transition of d-DctD₂ into the transcriptionally active state was achieved in a glucose-specific manner.

Therefore, we hypothesized the involvement of a component that is able to specifically sense the presence of glucose and then endow transcription activity to d-DctD₂. The mutants of *V. vulnificus* with mutation at the *crr* locus were then analyzed, including the strains carrying a deletion of IIA^{Glc} (Δcrr), a dephospho-form of IIA^{Glc} (*crr*_{H75Q}), and deletions of both *crr* and *dctD₂* ORFs (Δcrr ΔdctD₂). The maximal and basal expression levels of the two clusters were obtained in the Δcrr mutant grown in AB-fumarate and AB-glucose, respectively, which indicated that the effect of *crr* deletion on the expression of the two clusters was only observed in the cells grown in AB-glucose. In

addition, a double mutant produced basal levels of expression, which were the same levels as the $\Delta dctD_2$ mutant. Thus, the glucose-specific component involved in the above hypothetical regulatory pathway is IIA^{Glc}. Since the phosphorylated state of IIA^{Glc} is determined by glucose (39), it was assumed that d-IIA^{Glc} might influence the transcription activity of d-DctD₂. To test this assumption, the expression of the two clusters was examined using *crr*_{H75Q}. In AB-glucose, the *crr*_{H75Q} strain showed the maximal expression of two clusters, which were the same levels found in the *crr*_{H75Q} strain grown in AB-fumarate. These results suggested that d-DctD₂ became a transcriptionally active state if the cellular levels of d-IIA^{Glc} increased under growth conditions containing glucose.

Specific interaction of d-DctD₂ with d-IIA^{Glc}. IIA^{Glc} interacts with various proteins and regulates the activities of the target proteins (40, 41). Accordingly, we investigated the possibility of direct interaction between two proteins, d-IIA^{Glc} and d-DctD₂, since both accumulated in the cells under the glucose-rich condition. A β -galactosidase-based bacterial two-hybrid system (BACTH) (Euromedex) was utilized. Two plasmids, pUT18c and pKT25, containing *dctD₂* and *crr*, respectively, were cotransformed into *Escherichia coli*. The resultant transformant was spotted on M9-glucose or M9-phosphoenolpyruvate (PEP) agar plates supplemented with 40 μ g/mL X-Gal (5-bromo-4-chloro-3-indolyl- β -D-galactopyranoside) (Fig. 5A and C). For comparison, the negative and positive controls, which were *E. coli* harboring a combination of pUT18c and pKT25 vectors and a combination of pUT18c-*zip* and pKT25-*zip*, respectively, were also spotted on the same agar plates. Blue colonies of the cells carrying pUT18c-*dctD₂* and pKT25-*crr* formed on the M9-glucose plate, but not on the M9-PEP plate, which suggested that only d-IIA^{Glc} exhibited an affinity for DctD₂. The measured activities of β -galactosidase produced in M9-glucose and M9-PEP were the same as those of the positive control and negative control, respectively (Fig. 5B and D).

It was assumed that most DctD₂ proteins in cells grown in glucose, without any dicarboxylic acid, existed as d-DctD₂, based on a prior finding (42). To identify which form of DctD₂ participates in binding with d-IIA^{Glc}, *in vitro* binding assays were performed using various combinations of the two proteins (Fig. 5E). Native gel electrophoresis analysis revealed a novel band in samples with a combination of DctD_{D57Q} (d-DctD₂) with d-IIA^{Glc}. It indicated the formation of a complex of the two proteins, whose intensities were apparently dependent upon the concentration of each protein. However, a combination of DctD_{D57E} (p-DctD₂) with d-IIA^{Glc} did not produce any new band, suggesting that p-DctD₂ was not able to interact with d-IIA^{Glc} (the last lane in Fig. 5E).

d-DctD₂ specifically bound to the upstream region of the EPS-cluster if d-IIA^{Glc} was provided. Phosphorylation of bEBPs occurs prior to their binding to DNA (12). In the case of *V. vulnificus* DctD₂, which activates the transcription of EPS-II and EPS-III clusters, its phosphorylation state was suggested to result from kinase activity of the cognate sensors for dicarboxylic acids (16). However, in the presence of glucose, transcriptional activation of the EPS-II and EPS-III clusters required the presence of d-IIA^{Glc} and d-DctD₂ (Fig. 4). Both showed a specific interaction to form a complex (Fig. 5). Thus, we examined whether the complex of d-DctD₂ and d-IIA^{Glc} would interact with the regulatory region of the target genes by performing an electrophoretic mobility shift assay (EMSA) with three kinds of recombinant DctD₂: the original, wild-type (WT) DctD₂ (DctD_{WT}), DctD_{D57E} (p-DctD₂), and DctD_{D57Q} (d-DctD₂). They were individually added to the reaction mixtures containing 50 nM probe DNA covering the nucleotides from -418 to +62 relative to the transcription initiation site 1 (TIS-1) of the EPS-II gene cluster (Fig. 6). As previously reported, DctD_{WT} bound to the probe in a concentration-dependent manner (16) (Fig. 6A). It was presumed that the DctD_{WT} preparations used in this study contained both phosphorylated and dephosphorylated forms of DctD₂. Thus, the recombinant DctD₂ preparations including only one form (either p-DctD₂ or d-DctD₂) were added to the same DNA probe. p-DctD₂ began to bind the probe in the reaction mixture with the lowest concentration of DctD₂ (e.g., 100 nM), which had approximately 3 times higher affinity than DctD_{WT}, and the intensity of the bound probes increased as the added concentrations of p-DctD₂ increased up to 500 nM

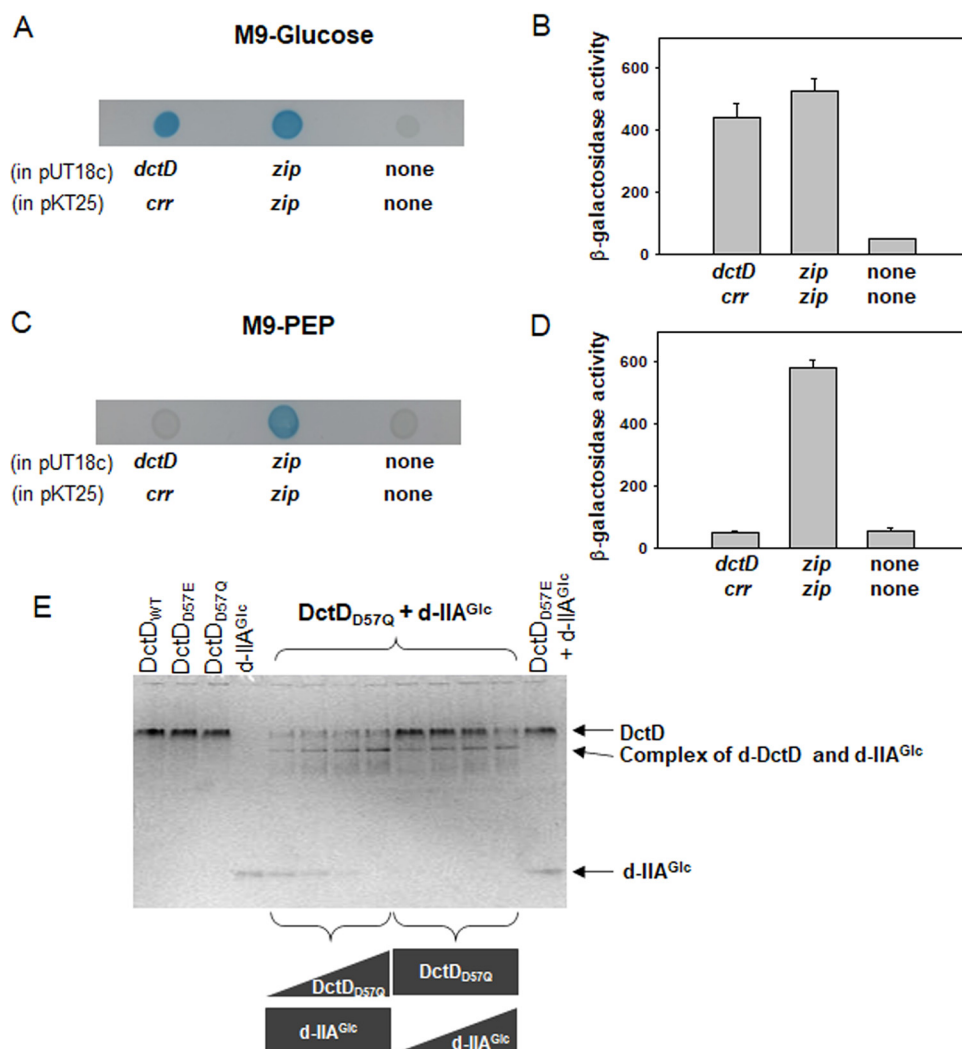


FIG 5 Specific interaction between DctD₂ and IIA^{Glc} proteins. (A to D) Bacterial two-hybrid system. Two plasmids, pUT18c-*dctD*₂ and pKT25-*crr* (Table S1), were constructed and cotransformed to *E. coli* BTH101, as described in Materials and Methods. This transformant was grown in M9 medium supplemented with glucose (Glc) (A and B) or phosphoenolpyruvate (PEP) (C and D), and then the resultant β -galactosidase activities were examined. For comparison, the negative and positive controls (*E. coli* BTH101 harboring pUT18c/pKT25 and pUT18c-*zip*/pKT25-*zip*, respectively), were included in these assays: shown are blue colonies on the agar plates supplemented with 40 μ g/mL X-Gal (A and C) and the specific β -galactosidase activities in Miller units (B and D), as described in Materials and Methods. (E) *In vitro* interaction between d-IIA^{Glc} and d-DctD₂. To examine the role of the phosphorylated states of DctD₂ in specific interaction with d-IIA^{Glc}, both phosphorylated (p-) and dephosphorylated (d-) forms of recombinant DctD₂ were prepared: the original DctD₂ (DctD_{WT}), p-DctD₂ (DctD_{D57E}), and d-DctD₂ (DctD_{D57Q}) (Table S1). Various combinations of DctD₂ and d-IIA^{Glc} proteins were mixed, and the reaction mixtures were run in a native gel. Lane 1, DctD_{WT} (5 μ M); lane 2, DctD_{D57E} (5 μ M); lane 3, DctD_{D57Q} (5 μ M); lane 4, d-IIA^{Glc} (5 μ M); lanes 5 to 8, d-IIA^{Glc} (5 μ M) with DctD_{D57Q} at a concentration of 0.04, 0.2, 1, or 5 μ M; lanes 9 to 12, DctD_{D57Q} (5 μ M) with d-IIA^{Glc} at a concentration of 0.04, 0.2, 1, or 5 μ M; and lane 13, DctD_{D57E} (5 μ M) with d-IIA^{Glc} (5 μ M). Each protein band and the newly emerged band are indicated with arrows.

(Fig. 6B). However, as expected, d-DctD₂ did not show any affinity for the same probe up to the highest concentration of DctD used in this study (e.g., 700 nM) (Fig. 6C). These results clearly demonstrate that d-DctD₂ has no DNA-binding affinity.

The same EMSA was performed in the presence of d-IIA^{Glc}. When the DNA probes mixed with various concentrations of DctD_{WT} were treated with 500 nM d-IIA^{Glc}, a slowly migrating band emerged in a concentration-dependent manner (Fig. 6D), in addition to a band of the probes bound by p-DctD₂ (Fig. 6A). We hypothesized that the d-DctD₂ fractions comprising the DctD_{WT} preparations can interact with d-IIA^{Glc} to

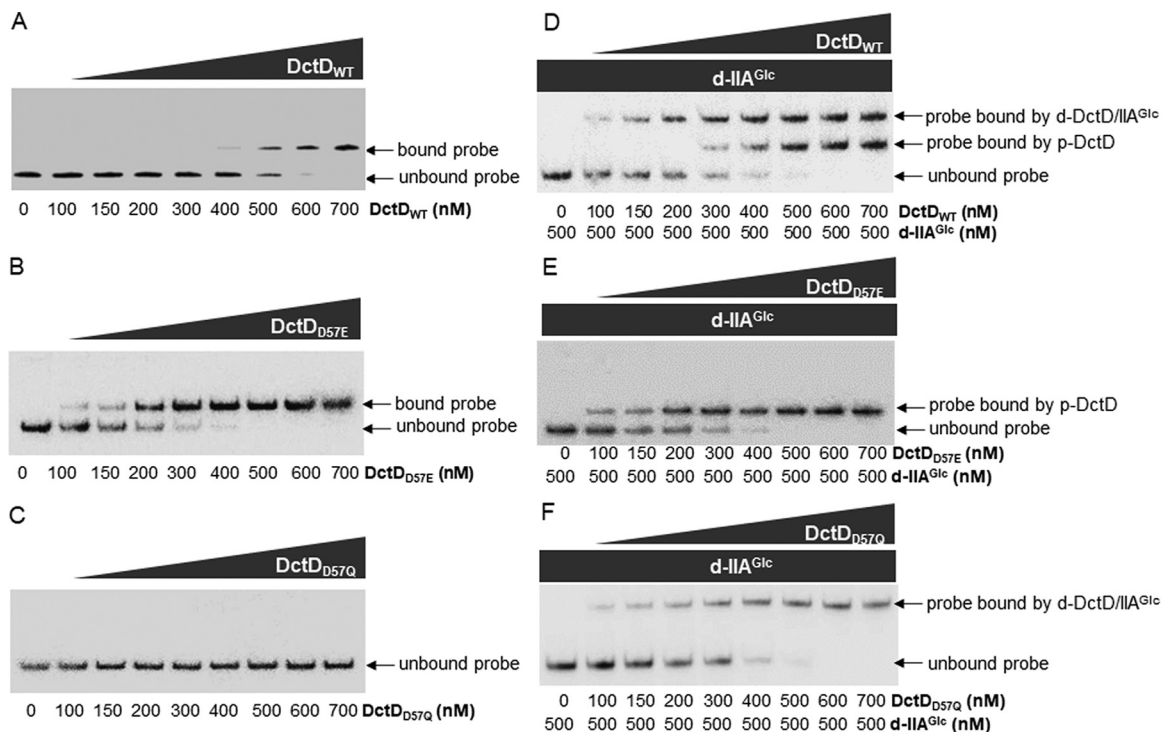


FIG 6 Binding affinities of p-DctD₂ and d-DctD₂/d-IIA^{Glc} complex to the regulatory region of the EPS-II cluster. The labeled DNA probe (50 nM), covering -391 to +61 relative to the TIS of the EPS-II gene cluster (16), was incubated with DctD_{WT} (A), DctD_{D57E} (B), and DctD_{D57Q} (C) at concentrations ranging from 100 to 700 nM. To examine the role of d-IIA^{Glc} in DNA binding of DctD, the same mixtures were also added with 500 nM d-IIA^{Glc} (D, E, and F). The reaction mixtures were resolved in 6% native polyacrylamide gels. Lane 1, probe only; and lanes 2 to 9, probe with DctD proteins at a concentration of 100, 150, 200, 300, 400, 500, 600, or 700 nM DctD_{WT}. DNA probes bound by p-DctD (A, B, D, and E) or a complex of d-DctD with d-IIA^{Glc} (D and F) are indicated with arrows.

form a complex that specifically binds to the probe DNA. To test this hypothesis, p-DctD₂ and d-DctD₂ were separately added to the reaction mixtures containing 50 nM DNA probes and 500 nM d-IIA^{Glc}. No slowly migrating band was evident in the reaction mixtures containing p-DctD₂ (Fig. 6E). However, the band indicating the probes bound by the complex of d-DctD₂ and d-IIA^{Glc} appeared in a d-DctD₂ concentration-dependent manner up to 500 nM (Fig. 6F). These results demonstrated that d-DctD₂, which was not able to bind DNA by itself, gained DNA-binding affinity not with its phosphorylation process, but through its binding with d-IIA^{Glc}.

Cellular levels of DctD₂ and IIA^{Glc} in *V. vulnificus* cells grown in fumarate, glucose, mannose, or glycerol. Expression of the transcriptional reporters for *ntrC* and *dctD₂* genes was highly induced in *V. vulnificus* cells grown in AB-fumarate and AB-glucose, compared to the cells grown in AB-mannose or AB-glycerol (Fig. 3A). To monitor the cellular levels of DctD₂, *V. vulnificus* cells were harvested at the exponential phase (at an optical density at 595 nm [OD₅₉₅] of 0.4) in each growth medium. Western blot analysis using anti-DctD₂ antibodies revealed that approximately 4.5-times-higher levels of DctD₂ were present in the cells grown in AB-fumarate and AB-glucose than in AB-mannose and AB-glycerol (Fig. 7A and D). These results were consistent with the expression patterns of the *dctD₂*-reporter in each growth medium (Fig. 3B). Although the total levels of DctD₂ were similarly higher in the cells grown in the AB-fumarate and AB-glucose, most DctD₂ proteins were presumed to be the dephosphorylated form in the AB-glucose-grown cells. Next, the cellular abundance of d-IIA^{Glc} in cells grown in various carbon sources was further monitored. As expected from previous reports in many bacterial species (43), the cells grown in AB-glucose contained only d-IIA^{Glc} (Fig. 7B and E). In contrast, the cells grown in the presence of fumarate, mannose, or glycerol contained both d-IIA^{Glc} and p-IIA^{Glc} at ratios of 1:2.5, 1:2.4, or 1:2.5, respectively. These results support our interpretation of high expression of the EPS clusters in

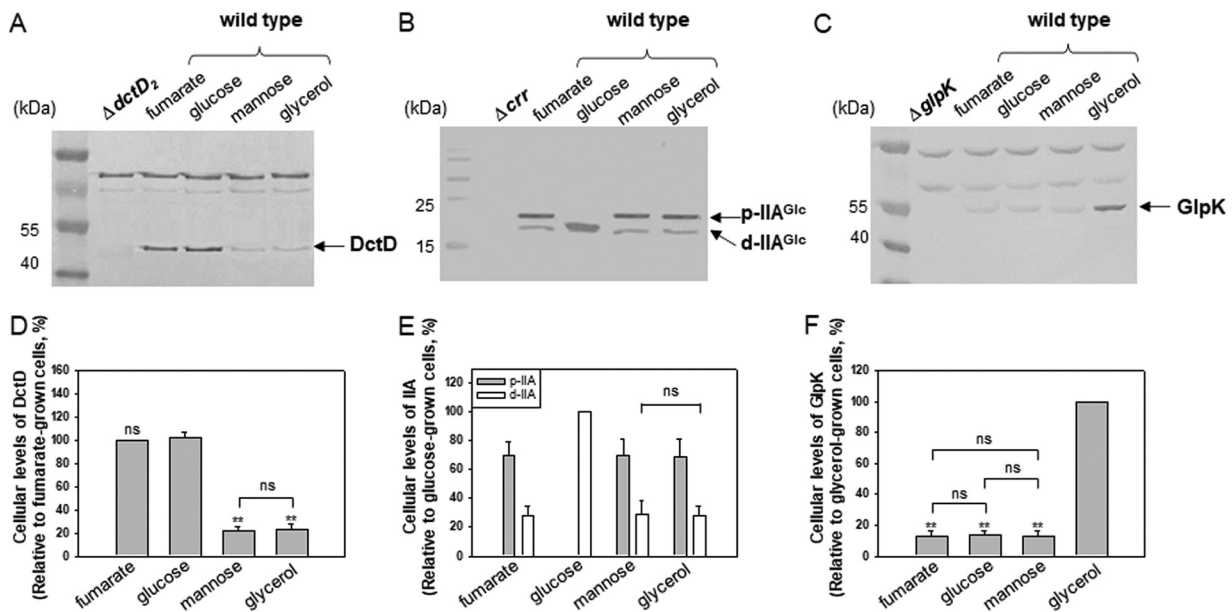


FIG 7 Cellular levels of DctD₂, IIA^{Glc}, and GlpK proteins in *V. vulnificus* cells grown in fumarate, glucose, mannose, or glycerol. Protein levels of DctD₂ (A), IIA^{Glc} (B), and GlpK (C) in wild-type *V. vulnificus* cells, which were freshly grown in AB-fumarate, -glucose, -mannose, or -glycerol medium (up to an OD₅₉₅ of 0.4), were compared by Western blot analysis. For SDS-PAGE, 120, 20, and 50 μg of cell lysates were loaded to detect bands of DctD₂, IIA^{Glc}, and GlpK, respectively. As a negative control for each blot, lysates of the *dctD*, *crr*, or *glpK* deletion mutants were included. The intensities of the corresponding protein bands on each blot were quantified, and their relative amounts (normalized by the intensities of DctD₂ in cells grown in AB-fumarate [D], IIA^{Glc} in cells grown in AB-glucose [E], and GlpK in cells grown in AB-glycerol [F]) were plotted, with *P* values indicated as follows: **, *P* < 0.001; ns, not significant.

the presence of glucose, in which increased levels of d-IIA^{Glc} would suffice for the complex formation occurring with increased d-DctD₂, which could then activate transcription of the clusters.

Increased levels of GlpK in *V. vulnificus* cells grown with glycerol. Comparative analyses of the cellular levels of DctD₂ and IIA^{Glc} revealed similar levels in *V. vulnificus* cells grown in mannose and glycerol (Fig. 7A and B). Interestingly, expression of the EPS-II and -III clusters (Fig. 2B and C), production of EPS (Fig. 1D), and formation of biofilms (Fig. 1B) were significantly lower in the cells grown in AB-glycerol than in AB-mannose. These observations suggested the presence of a factor inhibiting d-DctD₂/d-IIA^{Glc} complex-mediated transcription of the EPS clusters, especially in cells grown with glycerol. Since it has been previously reported that the glycerol uptake system, such as GlpFK (44), is highly induced in the presence of glycerol (45), the cellular levels of GlpK were monitored in the cells grown using various carbon sources. Significantly increased levels of GlpK were observed in cells grown in glycerol, which were approximately 7.5 times higher than the levels of GlpK in cells grown in fumarate, glucose, or mannose (Fig. 7C and F).

The direct interaction between GlpK and d-IIA^{Glc} has been described in *E. coli* (46). This might compete with the interaction between d-DctD₂ and d-IIA^{Glc}. Thus, to further investigate the effect of increased GlpK on the levels of d-IIA^{Glc} that would interact with d-DctD₂, it was first examined whether *V. vulnificus* GlpK would interact with IIA^{Glc} (see Fig. S2A in the supplemental material). As shown in *E. coli*, two proteins of *V. vulnificus* also exhibited strong binding affinity to form a complex. Next, the possibility of direct interaction of GlpK with DctD₂ was examined, but no interaction between these two proteins was revealed (Fig. S2B). These results might explain the lowest expression of the EPS gene clusters in *V. vulnificus* cells grown with glycerol, due to the increased GlpK, which in turn decreased the cellular levels of the free d-IIA^{Glc} available for complex formation with d-DctD₂.

DNA-binding affinity of the d-DctD₂/d-IIA^{Glc} complex was inhibited by GlpK. The observations that d-IIA^{Glc} was able to form complexes with d-DctD₂ (Fig. 5E) and GlpK (Fig. S2A) prompted a further examination of whether the formation of the d-IIA^{Glc}/

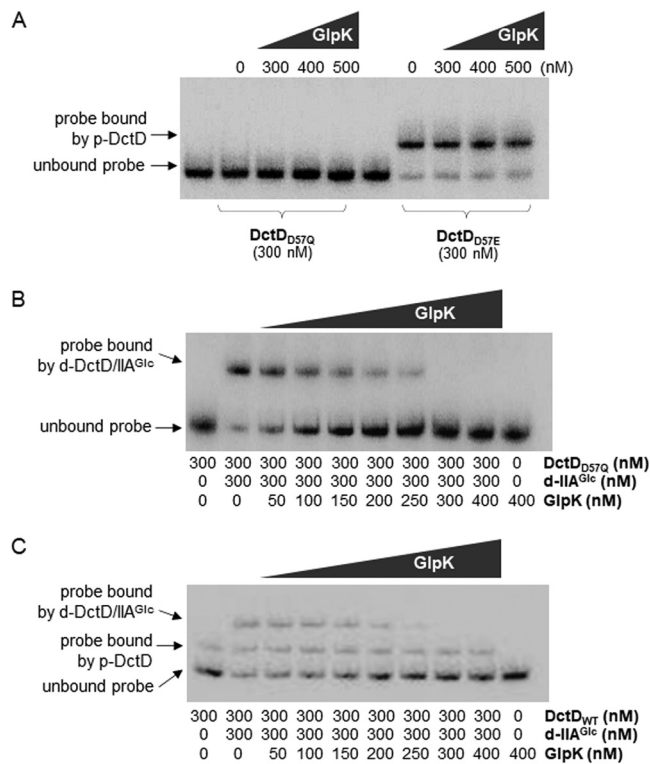


FIG 8 Effect of GlpK on the binding ability of the d-DctD₂/d-IIA^{Glc} complex to DNA probe. (A) Addition of GlpK to the probe mixed with d-DctD₂ or p-DctD₂. Labeled DNA probes (50 nM), used in Fig. 6, were mixed with either 300 nM DctD_{D57Q} (lanes 3 to 5) or 300 nM DctD_{D57E} (lanes 8 to 10). To examine the effect of GlpK on the interaction of DctD₂ and DNA probe, various concentrations of recombinant GlpK ranging from 300 to 500 nM were added, and then the reaction mixtures were resolved in a 6% native polyacrylamide gel. Lanes 1 and 6, DNA probe only; and lanes 2 and 7, DNA probe with 300 nM DctD₂. Unbound DNA and the probes bound by p-DctD₂ are indicated with arrows. (B) Addition of GlpK to the probe mixed with d-DctD and d-IIA^{Glc}. Labeled DNA probes (50 nM) mixed with 300 nM DctD_{D57Q} and 300 nM d-IIA^{Glc} were further mixed with various concentrations of recombinant GlpK ranging from 50 to 400 nM (lanes 3 to 9). The reaction mixtures were resolved in a 6% native polyacrylamide gel. Lane 1, DNA probe with DctD_{D57Q} (300 nM); lane 2, DNA probe with DctD_{D57Q} (300 nM) and d-IIA^{Glc} (300 nM); and lane 10, DNA probe with GlpK (400 nM). Unbound DNA and the probes bound by a complex of d-DctD₂ and d-IIA^{Glc} are indicated with arrows. (C) Addition of GlpK to the probe mixed with DctD_{WT} and d-IIA^{Glc}. Labeled DNA probes (50 nM), mixed with 300 nM DctD_{WT} (which included both d-DctD₂ and p-DctD₂) and 300 nM d-IIA^{Glc}, were further mixed with various concentrations of recombinant GlpK ranging from 50 to 400 nM (lanes 3 to 9). The reaction mixtures were resolved in a 6% native polyacrylamide gel. Lane 1, DNA probe with DctD_{WT} (300 nM); lane 2, DNA probe with DctD_{WT} (300 nM) and d-IIA^{Glc} (300 nM); and lane 10, DNA probe with GlpK (400 nM). DNA probes bound by p-DctD₂ or a complex of d-DctD₂ with d-IIA^{Glc} are indicated with arrows.

GlpK complex would interfere with the formation of d-IIA^{Glc}/d-DctD₂ by examining the behavior of the d-IIA^{Glc}/d-DctD₂ complex in response to the target DNA probe in the presence of various concentrations of GlpK. It was first checked if GlpK would affect the DNA-binding affinity of both forms of DctD₂ in the absence of d-IIA^{Glc}, but GlpK did not cause any change in the DNA-binding affinity of both forms of DctD₂ (Fig. 8A). However, in the presence of added GlpK, the amount of DNA probe bound by the d-IIA^{Glc}/d-DctD₂ complex was apparently decreased in a GlpK concentration-dependent manner, with a coincidental increase in the intensities of the unbound probe (Fig. 8B). The DNA probes bound by the complex completely disappeared in the reaction mixtures containing GlpK at concentrations equal to or greater than those of d-IIA^{Glc} and d-DctD₂ (≥ 300 nM). As expected from the specificity of the interaction of GlpK with d-IIA^{Glc}, the band intensities of DNA probes bound by p-DctD₂ were not affected by the addition of GlpK (Fig. 8C). In contrast, the band intensities of DNA probes bound by the d-IIA^{Glc}/d-DctD₂ complex were affected by the addition of GlpK, and the bands

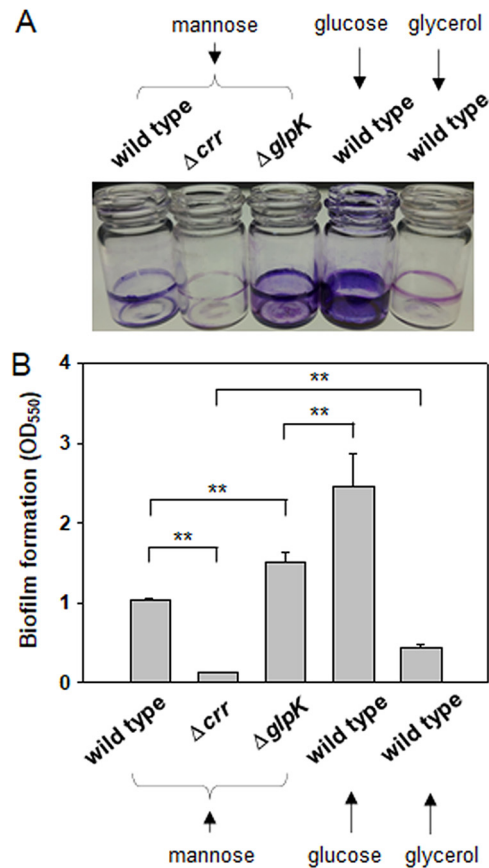


FIG 9 Biofilm formation by Δcrr and $\Delta glpK$ mutant strains of *V. vulnificus* in the presence of mannose. The wild-type and Δcrr and $\Delta glpK$ mutant strains were statically incubated for 48 h in AB medium supplemented with mannose, and the resultant biofilms on the borosilicate tubes were estimated by staining with crystal violet (A). For comparison, biofilms formed by the wild type in AB medium supplemented with glucose or glycerol were included. The associated dyes were dissolved and measured by spectrophotometry at 550 nm (B). The *P* values are indicated above corresponding horizontal lines: **, *P* < 0.001; *, 0.001 ≤ *P* < 0.01; ns, not significant.

eventually disappeared in the presence of higher concentrations of GlpK. The findings from all the experiments using GlpK support the hypothesis that GlpK inhibits the formation of a transcriptionally active form of d-DctD₂, especially in cells grown under glycerol-enriched conditions.

Biofilm formation by mutants defective in IIA^{Glc} or GlpK. To verify the *in vivo* effect derived from the competitive relationship between d-DctD₂ and GlpK in forming a complex with d-IIA^{Glc} (Fig. 8), one of the *V. vulnificus* phenotypes related to the degree of expression of the EPS gene clusters was examined. Since maturation of biofilms is tightly dependent upon EPS production (28, 31), the extents of mature biofilms developed by *V. vulnificus* wild-type and Δcrr and $\Delta glpK$ mutant strains were compared in AB-mannose (i.e., in the absence of glucose and glycerol) (Fig. 9A). Biofilm formation by the wild type in AB-mannose was approximately 2.1 times lower than that in AB-glucose and 3.4 times higher than that in AB-glycerol (Fig. 9B). These values were intermediate among the degrees of biofilm formation in AB-glucose and AB-glycerol media (as shown in Fig. 1A and B), which could be supported by the expression results of the EPS-II and EPS-III clusters in AB-mannose (as shown in Fig. 2B and C). Deletion of the *crr* gene encoding IIA^{Glc} resulted in a basal level of biofilm formation, which was slightly but significantly lower than the level of biofilm formation by the wild type in glycerol, due to the absence of a factor transforming the transcriptionally inactive d-DctD₂ into the transcriptionally active d-DctD₂/d-IIA^{Glc} complex. In contrast, biofilms

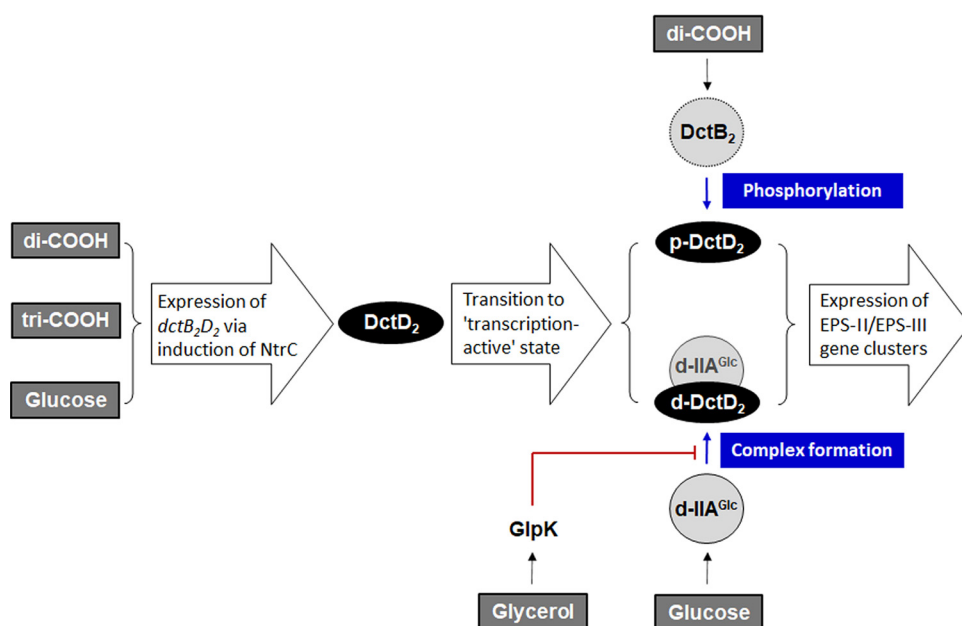


FIG 10 DctD₂-directed regulatory pathways for expression of two gene clusters for EPS-II/III biosynthesis in response to various carbon sources. Production of EPS, which is essential for *V. vulnificus* to mature biofilms, is controlled at the level of transcription of the gene clusters for EPS biosynthesis (EPS clusters). Thus, the cellular abundance of transcriptionally active forms of DctD₂ responsible for regulating the EPS-II and EPS-III clusters (16) determines the degrees of EPS production and biofilm maturation. Transcription of *dctD₂* is activated by NtrC, whose expression is induced under conditions with TCA intermediates (i.e., di- and tricarboxylic acids) (16) and glucose. In the presence of dicarboxylic acids, most DctD₂ is present in the transcriptionally active state as a phosphorylated form (p-DctD₂) by its cognate sensor kinase DctB₂ (42). The transcriptionally inactive, dephosphorylated form of DctD₂ (d-DctD₂) is capable of activating the transcription of EPS gene clusters in cells grown with glucose, in which d-DctD₂ forms a complex with d-IIA^{Glc}. This d-DctD₂-mediated transcription of the EPS-gene clusters is reduced in the presence of glycerol, due to a competitive inhibition of GlpK against the formation of the d-DctD₂/d-IIA^{Glc} complex.

formed by the $\Delta glpK$ mutant in AB-mannose were significantly increased compared to those by the wild type grown in the same medium, possibly because of the increased fraction of free d-IIA^{Glc} capable of forming a complex with d-DctD₂ in the $\Delta glpK$ mutant. However, these levels were significantly lower than biofilms formed by the wild type grown in AB-glucose, in which both d-DctD₂ and d-IIA^{Glc} were significantly increased (Fig. 7A and B).

DISCUSSION

It has been considered that the transcriptionally active form of enhancer-binding response regulators belonging to TCS is in the phosphorylated state, which is achieved by their cognate sensor kinases under specific conditions (12). In addition to the signal transduction mechanism via phospho-relay, this study further identified a novel regulatory pathway to activate transcription, which is mediated by the dephosphorylated form of a response regulator without involvement of its cognate sensor kinase, as schematically summarized in Fig. 10. One of the well-known response regulators, DctD₂, is present in the phosphorylated and active form when bacterial cells are grown in the presence of dicarboxylic acids (16). However, upon growth in the presence of glucose, the dephosphorylated form of DctD₂ is able to efficiently activate the transcription of EPS gene clusters in a dicarboxylic acid-independent manner (Fig. 2 and 4). This glucose-dependent transition of d-DctD₂ from a transcriptionally inactive to transcriptionally active state, evidenced by the acquisition of DNA-binding ability (as shown in Fig. 6), necessitates the involvement of another cellular factor indicating the availability of glucose in the ambient environment. Components of the glucose PTS are mostly present in the dephosphorylated states in bacterial cells growing in the presence of

glucose (47) (Fig. 7B), and d-IIA^{Glc} has been shown to specifically interact with d-DctD₂ (Fig. 5). Since p-DctD₂ would be in the multimeric states in order to bind to DNA, as shown in other members of the NtrC family (12), it was further speculated that a multimeric conformation of the d-IIA^{Glc}/d-DctD₂ complex might be involved in direct binding to DNA. This speculation could be supported by the observation that a DNA probe bound by the d-IIA^{Glc}/d-DctD₂ complex showed more retarded mobility than the same DNA probe bound by p-DctD₂ (Fig. 6D).

In addition to the role of the glucose PTS in translocating glucose molecules into the cytoplasm in a phosphorylated form (glucose-6-phosphate), its components are versatile proteins that interact with diverse proteins and regulate their cellular functions (41). In the case of IIA^{Glc} relaying the phosphate group from HPr to IIBC^{Glc}, it has been further reported that IIA^{Glc} specifically interacts with enzymes (Cya, FrsA, AraG, MalK, and GlpK), non-PTS transporters (LacY, GalP, MelB, and RafB), and chemotactic signal transducers (CheW) in several bacterial species (48–50). Besides these proteins targeted by IIA^{Glc}, some transcription factors are affected by other components of the glucose PTS. The membrane-bound IIB^{Glc} binds to a transcription factor, Mlc, and then sequesters it from its transcription regulation of the target genes in *E. coli* (51), and HPr makes MtlR an active transcription factor by direct phosphorylation in *Bacillus subtilis* (52). The present study demonstrates that IIA^{Glc} can form a complex with the inactive DctD₂ and convert it to an active DctD₂ having the DNA-binding affinity. This is the first evidence that the interaction of IIA^{Glc} with a transcription factor results in an effect mimicking the phosphorylated form of a response regulator.

As mentioned above, d-IIA^{Glc} was able to form a complex with glycerol kinase, GlpK (Fig. S2A). This led us to speculate that GlpK plays a role in the expression of genes regulated by the d-DctD₂/d-IIA^{Glc} complex, especially under conditions that enrich the cellular abundance of GlpK. Cellular levels of GlpK were highly induced in cells grown in AB-glycerol medium (Fig. 7C), and GlpK might outcompete d-DctD₂ in forming the complex with d-IIA^{Glc}. As a result, the potential to form the d-DctD₂/d-IIA^{Glc} complex was presumed to be lowered in the cells growing with glycerol compared to the cells growing with mannose (Fig. 7B). This competitive interaction between d-DctD₂ and GlpK was evidenced *in vitro* by EMSA (Fig. 8). Furthermore, when comparing the intensities of the probes bound by various concentrations of the d-DctD₂/d-IIA^{Glc} complex (Fig. 6F) with those in the presence of various amounts of added GlpK (Fig. 8B), the binding affinity of GlpK to d-IIA^{Glc} appeared to be slightly higher than that of d-DctD₂ to d-IIA^{Glc}. The *in vivo* effect caused by the increased levels of GlpK was confirmed by observing the biofilm phenotype of the $\Delta glpK$ mutant. This mutant exhibited the ability to form significantly increased biofilms in AB-mannose medium compared to the wild type in the same growth medium (Fig. 9).

Both the production of EPS and the formation of mature biofilms were greatly increased when cells were grown in the presence of glucose (Fig. 1). These processes were accomplished by sequential induction of *ntrC* and *dctD₂* gene expression (Fig. 3), accumulation of d-IIA^{Glc} (Fig. 7B), complex formation of d-DctD₂ with d-IIA^{Glc} (Fig. 5), and transcriptional activation of the gene clusters for EPS biosynthesis (Fig. 2 and 4). NtrC is the main transcription factor activating the *dctB₂D₂* operon in *V. vulnificus* (16). Induction of NtrBC via sensing the cellular fluctuations of glutamate (Glu) and glutamine (Gln) as a carbon/nitrogen ratio has been documented. In the cells growing with the tricarboxylic acid (TCA) intermediates (i.e., tri- and dicarboxylic acids), the activities of α -ketoglutarate (α -KG) dehydrogenase, catalyzing conversion of α -KG to succinyl coenzyme A (succinyl-CoA), and succinate dehydrogenase, catalyzing conversion of succinate to fumarate, are inhibited. Then, the increased cellular levels of α -KG result in increased levels of Glu, which activates NtrBC (53–55). Under glucose-rich conditions, the cellular levels of cAMP are minimal, resulting in relief of the repression of the *ntr* operon by the cAMP-cAMP receptor protein (CRP) complex (56). Therefore, under conditions that result in increased levels of NtrC (e.g., TCA intermediates or glucose), the expression of DctD₂ is highly induced. The induced cellular level of DctD₂ is not the

only requirement for maximal activation of the EPS gene clusters' transcription. DctD₂ needs to be converted to the transcriptionally active state: the p-DctD₂ is formed in the presence of dicarboxylic acids among the TCA intermediates (16), and the d-DctD₂/d-IIA^{Glc} complex is formed in the presence of glucose (Fig. 5A).

This series of regulations of EPS production may be disrupted by glycerol. It is conceivable that the addition of glycerol might reduce the gluconeogenesis process producing the key sugars of EPS and/or the other processes catalyzing carbon storage in the form of carbon-rich polymers. As evidenced by the highly induced expression of GlpK by glycerol (Fig. 7C) and its antagonistic effect on the formation of the d-DctD₂/d-IIA^{Glc} complex (Fig. 8), GlpK could play an important role in guaranteeing the reduced expression of EPS gene clusters, even in cells with some amounts of d-DctD₂ and d-IIA^{Glc}. DctD₂ in *V. vulnificus* cells growing in AB-glycerol should be in the dephosphorylated state, but their IIA^{Glc} proteins are present in both forms, p-IIA^{Glc} and d-IIA^{Glc} (Fig. 7B). Thus, the cellular levels of d-IIA^{Glc} available to form a complex of d-DctD₂ with d-IIA^{Glc} should be limited in the cells growing in AB-glycerol medium, due to the increased levels of GlpK. As a result, these cells showed a significantly decreased ability to produce EPS and form biofilms compared to the cells growing in AB-mannose medium (Fig. 1 and 2). Similarly, other non-PTSs might have the same inhibitory effect. The inhibitory effect of GlpK, with higher affinity than d-DctD₂, might suggest a role similar to that of other non-PTS transporters, guaranteeing the reduced expression of EPS gene clusters. In addition to the role of glycerol in the inhibition of d-DctD₂/d-IIA^{Glc} complex formation via the involvement of GlpK, the other carbon sources could have the same effect as glycerol, if their kinases are able to interact with d-IIA^{Glc}: for example, maltose and its kinase, MalK (57), or arabinose and its kinase, AraG (58).

Production of EPS and formation of mature biofilms are important for increased colonization and survival of *V. vulnificus* in various environments, including its hosts. Since EPS biosynthesis is regulated at the level of transcription in *V. vulnificus* (28), the fine-tuned regulation of EPS biosynthesis is required to sense the ambient environmental parameters, such as the types of carbon sources, and to initiate and prepare a biofilm lifestyle. Transcription initiation activated by bEBP, such as DctD, occurs in RpoN-dependent TIS (12). As previously reported (16), the gene clusters for EPS-II and EPS-III have both RpoN-dependent TIS (TIS-1) and RpoD-dependent TIS (TIS-2). The observations of the effects of carbon sources on the DctD₂-mediated activation shown in this study are the results of the induction at TIS-1 of each cluster. The transcription of the EPS-II gene cluster (also called the *brp* operon) can be induced at its TIS-2 by the c-di-GMP-responding transcription factors BrpR and BrpT (30, 59).

This study demonstrates that the foodborne pathogen *V. vulnificus* utilizes both dicarboxylic acids and glucose as the specific signals to turn on the transcription of the EPS gene clusters and the sources to supply the monomeric constituents or their precursors for EPS polymerization, but efficiently adopts the differential pathways using a common response regulator, DctD₂, in the form of p-DctD₂ or d-DctD₂/d-IIA^{Glc} complex. These findings reveal a novel regulatory mechanism for EPS biosynthesis in glucose-enriched environments, which foodborne pathogens might encounter upon entry into the gastrointestinal tracts of hosts. The pathway mediated by the d-DctD₂/d-IIA^{Glc} complex is further delicately regulated by other carbon sources, such as glycerol, via the competitive action of their kinases inhibiting the formation of the d-DctD₂/d-IIA^{Glc} complex.

MATERIALS AND METHODS

Bacterial strains and culture conditions. All the strains and plasmids used in this study are separately listed in Table S1 in the supplemental material. The *E. coli* strains used for plasmid DNA preparation and for conjugational transfer were grown at 37°C in Luria-Bertani (LB) medium. *V. vulnificus* strains were grown at 30°C in AB medium (300 mM NaCl, 50 mM MgSO₄, 0.2% vitamin-free Casamino Acids, 10 mM potassium phosphate or 100 mM sodium phosphate, 1 mM L-arginine, pH 7.5) (60) supplemented with various carbon sources: fumarate (50.0 mM), glucose (33.4 mM), mannose (33.4 mM), or glycerol (66.7 mM). Antibiotics were added to LB or AB media at the following concentrations: for *E. coli*, ampicillin at 100 μg/mL, chloramphenicol at 20 μg/mL, kanamycin at 50 μg/mL, and tetracycline at 15 μg/mL, and for *V. vulnificus*, chloramphenicol at 2 μg/mL and tetracycline at 3 μg/mL.

Biofilm formation assay. Wild-type and mutant strains of *V. vulnificus* were freshly inoculated to the AB media supplemented with various carbon sources in borosilicate tubes and statically incubated at 30°C. At 48 h, the planktonic phases were removed from the tubes, and their cell densities were measured by spectrometric reading at OD₅₉₅ to check the appropriate growth of cells on the specific carbon sources. Biofilms formed on tubes were washed twice with phosphate-buffered saline (PBS: 100 mM NaCl, 20 mM sodium phosphate [pH 7.5]) (61), and then the remaining biofilms were stained with 1.0% crystal violet. After briefly washing out the dyes unassociated with biofilms in the tubes with distilled water (DW), the biofilm-associated dyes were eluted in ethanol. The resultant elution was diluted, if necessary, and subjected to spectrometry to estimate OD₅₅₀ (62).

Extraction and analysis of EPS. *V. vulnificus* cells were grown on AB agar plates supplemented with various carbon sources for 48 h, and then the produced EPSs were extracted and quantified, as previously described (28, 63). The fractions of loosely associated extracellular matrix were eluted in PBS and sequentially treated with a mixture of RNase A (50 μg/mL), DNase I (50 μg/mL), and MgCl₂ (10 mM) for 12 h and then with proteinase K (200 μg/mL) for 8 h. The fractions of polysaccharides remaining in the reaction mixture were treated with phenol-chloroform (1:1 [vol/vol]), and the resultant extracts were treated with sodium acetate (300 mM) to precipitate polysaccharides in the presence of 2.5× volumes of ethanol. The precipitates were washed with 70% ethanol and then resuspended in appropriate volumes of DW based upon the bacterial biomasses used for the EPS extraction: i.e., 100 μL of DW per OD₅₉₅ of 50. Aliquots of EPS fractions were run on a 5% stacking polyacrylamide gel, as described previously (28), and visualized with Stains-All (Sigma). The carbohydrate contents in each EPS fraction were estimated by the phenol-sulfuric acid method, using glucose as a carbohydrate standard (64), to present the concentrations of EPS as the glucose equivalents (Glc-eq.).

Measurement of transcriptional reporter plasmids fused with the luciferase genes. The *luxAB*-based transcription reporters, previously described (16, 28), were mobilized to various strains of *V. vulnificus*. The intensities of the light produced by the cells grown in the presence of specific carbon sources were measured with a luminometer (TD-20/20 luminometer; Turners Designs), after the bacterial culture aliquots were mixed with a luciferase substrate (e.g., *n*-decyl aldehyde [0.006%]). Specific bioluminescence was presented by normalizing the relative light units (RLU) with respect to cell mass (OD₅₉₅), as described previously (65).

Construction of mutant strains of *V. vulnificus*. For construction of the Δ *glpK* mutant, a suicide vector, pDM4 (66), was ligated with a DNA fragment containing the deleted ORFs of *glpK*, which was produced by using two sets of primers: (i) *GlpK*-upF and *GlpK*-upR and (ii) *GlpK*-downF and *GlpK*-downR (see Table S2 in the supplemental material). pDM4- Δ *glpK* was transformed into *E. coli* SM10 λ *pir*, and the resultant transformant was conjugated with *V. vulnificus*. The exconjugants were selected on the appropriate agar plate (i.e., thiosulfate citrate bile sucrose medium supplemented with 3 μg/mL chloramphenicol). Then, an isolated colony with the characteristics indicating a double homologous recombination event (67) was examined by PCR using primers *GlpK*-upF and *GlpK*-downR (Table S2) to confirm the mutation in its *glpK* locus. Mutation in Δ *glpK* was further examined via complementation of the mutant with pRK415 containing the intact *glpK* amplified using primers *GlpFK*-comF and *GlpFK*-comR (Table S2).

For construction of the mutants whose *dctD*₂ and/or *crr* genes were site-directedly mutagenized, various DNA fragments encompassing these ORFs were prepared by the overlap extension method (68), using appropriate sets of primers (Table S2). For convenience in isolating the mutant among the conjugation mixtures, modified nucleotide sequences for a restriction enzyme were artificially generated in the vicinity of the mutation site without alteration of the original amino acid sequences. For example, the DNA fragments of *dctD*_{D57E} and *dctD*_{D57Q} were produced using the internal primer sets D57E_Agel-F and D57E_Agel-R and D57Q_Agel-F and D57Q_Agel-R, respectively, including the substituted nucleotide sequences for the altered 57th codon and the restriction site of *Agel*. Similarly, *crr*_{H75Q} was produced using the internal primer set H75Q_SacI-F and H75Q_SacI-R. Site-directed mutagenized DNA fragments were then cloned to pDM4 to produce pDM4-*dctD*_{D57E}, pDM4-*dctD*_{D57Q}, and pDM4-*crr*_{H75Q}, which were transferred to *V. vulnificus* via conjugation and eventually exchanged with the original ORFs in the *V. vulnificus* genomes, as described above. Mutations in the target genes were examined by digestion of amplified DNA with the appropriate restriction enzymes (*Agel* for *dctD*_{D57E} and *dctD*_{D57Q} and *SacI* for *crr*_{H75Q}).

Bacterial two-hybrid assay. Two plasmids, pUT18c and pKT25, provided in the bacterial two-hybrid (BACTH) system (Euromedex) were inserted with *dctD*₂ and *crr*, respectively, and cotransformed into *E. coli* BTH101. The resultant transformant was spotted on the 5 mM glucose- or 10 mM PEP-supplemented M9-X-Gal (40 μg/mL) agar plate containing ampicillin (100 μg/mL), kanamycin (50 μg/mL), and IPTG (isopropyl- β -D-thiogalactopyranoside; 1 mM). The colony color that developed due to the produced β -galactosidase activity was compared with those of the positive control (*E. coli* BTH101 carrying pUT18C-*zip*/pKT25-*zip*) and the negative control (*E. coli* BTH101 carrying containing pUT18c/pKT25). To quantify the degrees of protein-protein interactions in the cells grown in M9 broth with 5 mM glucose or 10 mM PEP, β -galactosidase assays were performed. Harvested cells were resuspended in Z buffer (60 mM Na₂HPO₄, 40 mM NaH₂PO₄, 10 mM KCl, 1 mM MgSO₄, and 50 mM mercaptoethanol) (69) and treated with 0.1% SDS and chloroform to prepare crude cell lysates. Appropriate amounts of lysates of cells that were determined by OD₅₉₅ were incubated with ONPG (*o*-nitrophenol- β -galactoside) at a concentration of 0.67 mg/mL, the reactions were stopped by addition of Na₂CO₃ solution, and their OD₄₂₀ values were measured. β -Galactosidase activity was presented as follows: 1 U = (OD₄₂₀ × 1,000)/(time × cell culture vol × OD₅₉₅) (69).

Cloning and purification of recombinant proteins. For preparation of recombinant GlpK (rGlpK), a 1,546-bp DNA fragment containing the complete *glpK* gene was produced using GlpK-F and GlpK-R, the ends of which contained BamHI and HindIII sites, respectively (Table S2). Utilizing these restriction sites, *glpK* DNA was cloned into pQE30 (Qiagen) and then transformed into *E. coli* JM109 (Promega). For preparation of three kinds of recombinant DctD₂ (rDctD₂)—e.g., the original DctD₂ (DctD_{WT}), p-DctD₂ (DctD_{D57E}), and d-DctD₂ (DctD_{D57Q})—the plasmids pQE30-*dctD*₂, pQE-*dctD*_{D57E}, and pQE30-*dctD*_{D57Q} were expressed in *E. coli* JM109 in the presence of 1 mM IPTG. Each recombinant protein was purified using a Ni²⁺-nitrilotriacetic acid (NTA) affinity column (Bio-Rad).

In vitro protein-protein interaction assay. The mutant rDctD₂ (DctD_{D57Q} and DctD_{D57E}) and rGlpK were mixed with the recombinant d-IIA^{Glc} in 20 μL of an assay solution (50 mM Tris-HCl [pH 8.0], 20 mM KCl, 50 mM MgCl₂, and 100 mM NaCl). Reaction mixtures were composed of various combinations of DctD_{D57Q} and d-IIA^{Glc}, whose concentrations of each protein ranged from 0.04 μM to 5.0 μM. After 30 min of incubation at 30°C, the mixtures were combined with a loading buffer (0.01% bromophenol blue, 0.5 M Tris-HCl [pH 6.8], 50% glycerol) (70) and then subjected to nondenaturing gel electrophoresis using a gel made of 12% native polyacrylamide and a running buffer including 40 mM Tris-glycine (pH 8.3). After electrophoresis, the gel was stained with Coomassie brilliant blue to observe a newly emerged band in addition to the bands presenting each recombinant protein.

Electrophoretic mobility shift assay. Gel shift assays were performed with the DNA probe (480 bp) covering the regulatory region of the EPS-II cluster, which was amplified using the primer sets EPSII-F and EPSII-R, as previously described (16). Produced DNA fragment was labeled with [³²P]ATP using T4 polynucleotide kinase (TaKaRa), and the resultant labeled probe (approximately 50 nM) was incubated in a reaction buffer (50 mM Tris-HCl [pH 8.0], 20 mM KCl, 50 mM MgCl₂, and 100 mM NaCl) with various concentrations of rDctD₂ (e.g., DctD_{WT}, DctD_{D57E}, and DctD_{D57Q}) in the absence and presence of d-IIA^{Glc} and GlpK. The reaction mixtures were resolved in 6% native polyacrylamide gels, and the unbound probe and the probes bound by rDctD₂ or DctD₂/d-IIA^{Glc} were visualized and analyzed using Personal Molecular Imager FX and Quantity One software (Bio-Rad).

Western blotting. Cell lysates of wild-type and mutant strains of *V. vulnificus* were prepared in Tris-buffered saline with Tween 20 (TBST: 150 mM NaCl, 50 mM Tris-HCl, and 0.1% Tween 20) and appropriate amounts of protein extracts (e.g., 120 μg for DctD₂, 20 μg for IIA^{Glc}, and 50 μg for GlpK Western blots) were used for SDS-PAGE. Blotted membranes were blocked with 5% skim milk-TBST, incubated with the polyclonal antibodies raised against each recombinant protein, and then treated with alkaline phosphatase (AP)-conjugated goat anti-mouse IgG (Jackson ImmunoResearch Laboratories, Inc.) for anti-DctD₂ antibodies or AP-conjugated goat anti-rat IgG (Jackson ImmunoResearch Laboratories, Inc.) for anti-IIA^{Glc} and anti-GlpK antibodies. Using a nitroblue tetrazolium and 5-bromo-4-chloro-3-indolyl phosphate system (Promega), the immunoreactive bands were visualized, and their relative intensities were quantified using a densitometer (Bio-Rad Gel Doc 2000 system).

Statistical analyses. Results are expressed as means ± standard deviations of data from at least three independent experiments. Statistical analysis was performed using Student's *t* test (Systat Program, SigmaPlot version 9; Systat Software, Inc.). *P* values are represented by asterisks: *, 0.001 ≤ *P* < 0.01; **, *P* < 0.001.

ACKNOWLEDGMENTS

This work was supported by grants from the National Research Foundation, Republic of Korea (NRF-2018R1A5A1025077 [Microbial Survival Systems Research Center] and NRF-2021R1A2B5B02002477).

We thank B. R. Jang and Y. C. Jung for valuable comments and S.-J. Chun for constructing a *crr* mutant.

We declare no conflict of interest.

REFERENCES

- Hoch JA, Silhavy TJ (ed). 1995. Two-component signal transduction. American Society for Microbiology, Washington, DC.
- Stock AM, Robinson VL, Goudreau PN. 2000. Two-component signal transduction. *Annu Rev Biochem* 69:183–215. <https://doi.org/10.1146/annurev.biochem.69.1.183>.
- Alves R, Savageau MA. 2003. Comparative analysis of prototype two-component systems with either bifunctional or monofunctional sensors: differences in molecular structure and physiological function. *Mol Microbiol* 48:25–51. <https://doi.org/10.1046/j.1365-2958.2003.03344.x>.
- Kelly DP, Shergill JK, Lu WP, Wood AP. 1997. Oxidative metabolism of inorganic sulfur compounds by bacteria. *Antonie Van Leeuwenhoek* 71:95–107. <https://doi.org/10.1023/a:1000135707181>.
- Letunic I, Copley RR, Schmidt S, Ciccarelli FO, Doerks T, Schultz J, Ponting CP, Bork P. 2004. SMART 4.0: towards genomic data integration. *Nucleic Acids Res* 32(Database Issue):D142–D144. <https://doi.org/10.1093/nar/gkh088>.
- Laub MT, Goulian M. 2007. Specificity in two-component signal transduction pathways. *Annu Rev Genet* 41:121–145. <https://doi.org/10.1146/annurev.genet.41.042007.170548>.
- Varughese KI. 2005. Conformational changes of Spo0F along the phosphotransfer pathway. *J Bacteriol* 187:8221–8227. <https://doi.org/10.1128/JB.187.24.8221-8227.2005>.
- Gardino AK, Kern D. 2007. Functional dynamics of response regulators using NMR relaxation techniques. *Methods Enzymol* 423:149–165. [https://doi.org/10.1016/S0076-6879\(07\)23006-X](https://doi.org/10.1016/S0076-6879(07)23006-X).
- Kern D, Volkman BF, Luginbühl P, Nohaile MJ, Kustu S, Wemmer DE. 1999. Structure of a transiently phosphorylated switch in bacterial signal transduction. *Nature* 402:894–898. <https://doi.org/10.1038/47273>.
- Lewis HA, Chen H, Edo C, Buckanovich RJ, Yang YY, Musunuru K, Zhong R, Darnell RB, Burley SK. 1999. Crystal structures of Nova-1 and Nova-2 K-homology RNA-binding domains. *Structure* 7:191–203. [https://doi.org/10.1016/S0969-2126\(99\)80025-2](https://doi.org/10.1016/S0969-2126(99)80025-2).

11. Gao R, Stock AM. 2009. Biological insights from structure of two-component proteins. *Annu Rev Microbiol* 63:133–154. <https://doi.org/10.1146/annurev.micro.091208.073214>.
12. Bush M, Dixon R. 2012. The role of bacterial enhancer binding proteins as specialized activators of s54-dependent transcription. *Microbiol Mol Biol Rev* 76:497–529. <https://doi.org/10.1128/MMBR.00006-12>.
13. Fernandez-Lopez R, Ruiz R, Cruz F, Moncalian G. 2015. Transcription factor-based biosensors enlightened by the analyte. *Front Microbiol* 6:648. <https://doi.org/10.3389/fmicb.2015.00648>.
14. Xu H, Kelly MT, Nixon BT, Hoover TR. 2004. Novel substitutions in the sigma54-dependent activator DctD that increase dependence on upstream activation sequences or uncouple ATP hydrolysis from transcriptional activation. *Mol Microbiol* 54:32–44. <https://doi.org/10.1111/j.1365-2958.2004.04246.x>.
15. Giblin L, Archdeacon J, O'Gara F. 1996. Regulation of dct genes in the *Rhizobium meliloti*-alfalfa interaction. *World J Microbiol Biotechnol* 12: 151–156. <https://doi.org/10.1007/BF00364679>.
16. Kang S, Park H, Lee KJ, Lee KH. 2021. Transcription activation of two clusters for exopolysaccharide biosynthesis by phosphorylated DctD in *Vibrio vulnificus*. *Environ Microbiol* 23:5364–5377. <https://doi.org/10.1111/1462-2920.15636>.
17. Sutherland IW. 2001. The biofilm matrix—an immobilized but dynamic microbial environment. *Trends Microbiol* 9:222–227. [https://doi.org/10.1016/S0966-842X\(01\)02012-1](https://doi.org/10.1016/S0966-842X(01)02012-1).
18. Lebeaux D, Ghigo JM, Beloin C. 2014. Biofilm-related infections: bridging the gap between clinical management and fundamental aspects of recalcitrance toward antibiotics. *Microbiol Mol Biol Rev* 78:510–543. <https://doi.org/10.1128/MMBR.00013-14>.
19. Watters C, Fleming D, Bishop D, Rumbaugh KP. 2016. Host responses to biofilm. *Prog Mol Biol Transl Sci* 142:193–239. <https://doi.org/10.1016/bs.pmbts.2016.05.007>.
20. Bordas MA, Balebona MC, Zorrilla I, Borrego JJ, Moriñigo MA. 1996. Kinetics of adhesion of selected fish-pathogenic *Vibrio* strains of skin mucus of gilt-head sea bream (*Sparus aurata* L.). *Appl Environ Microbiol* 62: 3650–3654. <https://doi.org/10.1128/aem.62.10.3650-3654.1996>.
21. Costerton JW, Stewart PS, Greenberg EP. 1999. Bacterial biofilms: a common cause of persistent infections. *Science* 284:1318–1322. <https://doi.org/10.1126/science.284.5418.1318>.
22. Yang L, Barken KB, Skindersoe ME, Christensen AB, Givskov M, Tolker-Nielsen T. 2007. Effects of iron on DNA release and biofilm development by *Pseudomonas aeruginosa*. *Microbiology (Reading)* 153:1318–1328. <https://doi.org/10.1099/mic.0.2006/004911-0>.
23. Flemming HC, Wingender J. 2010. The biofilm matrix. *Nat Rev Microbiol* 8: 623–633. <https://doi.org/10.1038/nrmicro2415>.
24. Lopez D, Vlamakis H, Kolter R. 2010. Biofilms. *Cold Spring Harb Perspect Biol* 2:a000398. <https://doi.org/10.1101/cshperspect.a000398>.
25. Jennings LK, Storek KM, Ledvina HE, Coulon C, Marmont LS, Sadovskaya I, Secor PR, Tseng BS, Scian M, Filloux A, Wozniak DJ, Howell PL, Parsek MR. 2015. Pel is a cationic exopolysaccharide that cross-links extracellular DNA in the *Pseudomonas aeruginosa* biofilm matrix. *Proc Natl Acad Sci U S A* 112:11353–11358. <https://doi.org/10.1073/pnas.1503058112>.
26. Gilbert P, Das J, Foley L. 1997. Biofilm susceptibility to antimicrobials. *Adv Dent Res* 11:160–167. <https://doi.org/10.1177/08959374970110010701>.
27. Farmer JJ, III. 1979. *Vibrio* ("Benecke") *vulnificus*, the bacterium associated with sepsis, septicemia, and the sea. *Lancet* 314:903. [https://doi.org/10.1016/S0140-6736\(79\)92715-6](https://doi.org/10.1016/S0140-6736(79)92715-6).
28. Kim HS, Park SJ, Lee KH. 2009. Role of NtrC-regulated exopolysaccharides in the biofilm formation and pathogenic interaction of *Vibrio vulnificus*. *Mol Microbiol* 74:436–453. <https://doi.org/10.1111/j.1365-2958.2009.06875.x>.
29. Guo Y, Rowe-Magnus DA. 2011. Overlapping and unique contributions of two conserved polysaccharide loci in governing distinct survival phenotypes in *Vibrio vulnificus*. *Environ Microbiol* 13:2888–2990. <https://doi.org/10.1111/j.1462-2920.2011.02564.x>.
30. Chodur DM, Rowe-Magnus DA. 2018. Complex control of a genomic island governing biofilm and rugose colony development in *Vibrio vulnificus*. *J Bacteriol* 200:e00190-18. <https://doi.org/10.1128/JB.00190-18>.
31. Jung YC, Lee MA, Lee KH. 2019. Role of flagellin-homologous proteins in biofilm formation by pathogenic *Vibrio* species. *mBio* 10:e01793-19. <https://doi.org/10.1128/mBio.01793-19>.
32. Kim HS, Lee MA, Chun SJ, Park SJ, Lee KH. 2007. Role of NtrC in biofilm formation via controlling expression of the gene encoding an ADP-glyceromanno-heptose-6-epimerase in the pathogenic bacterium, *Vibrio vulnificus*. *Mol Microbiol* 63:559–574. <https://doi.org/10.1111/j.1365-2958.2006.05527.x>.
33. Donlan RM, Costerton JW. 2002. Biofilms: survival mechanisms of clinically relevant microorganisms. *Clin Microbiol Rev* 15:167–193. <https://doi.org/10.1128/CMR.15.2.167-193.2002>.
34. Vestby LK, Grønseth T, Simm R, Nesse LL. 2020. Bacterial biofilm and its role in the pathogenesis of disease. *Antibiotics* 9:59. <https://doi.org/10.3390/antibiotics9020059>.
35. Wishart DS, Tzur D, Knox C, Eisner R, Guo AC, Young N, Cheng D, Jewell K, Arndt D, Sawhney S, Fung C, Nikolai L, Lewis M, Coutouly MA, Forsythe I, Tang P, Shrivastava S, Jeroncik K, Stothard P, Amegbey G, Block D, Hau DD, Wagner J, Miniaci J, Clements M, Gebremedhin M, Guo N, Zhang Y, Duggan GE, Macinnis GD, Weljie AM, Dowlatabadi R, Bamforth F, Clive D, Greiner R, Li L, Marrie T, Sykes BD, Vogel HJ, Querengesser L. 2007. HMDB: the human metabolome database. *Nucleic Acids Res* 35:D521–D526. <https://doi.org/10.1093/nar/gkl923>.
36. Vitko NP, Grosser MR, Khatri D, Lance TR, Richardson AR. 2016. Expanded glucose import capability affords *Staphylococcus aureus* optimized glycolytic flux during infection. *mBio* 7:e00296-16. <https://doi.org/10.1128/mBio.00296-16>.
37. Brückner R, Titgemeyer F. 2002. Carbon catabolite repression in bacteria: choice of the carbon source and autoregulatory limitation of sugar utilization. *FEMS Microbiol Lett* 209:141–148. <https://doi.org/10.1111/j.1574-6968.2002.tb11123.x>.
38. Deutscher J, Francke C, Postma PW. 2006. How phosphotransferase system-related protein phosphorylation regulates carbohydrate metabolism in bacteria. *Microbiol Mol Biol Rev* 70:939–1031. <https://doi.org/10.1128/MMBR.00024-06>.
39. Dörschug M, Frank R, Kalbitzer HR, Hengstenberg W, Deutscher J. 1984. Phosphoenolpyruvate-dependent phosphorylation site in enzyme III_{glc} of the *Escherichia coli* phosphotransferase system. *Eur J Biochem* 144: 113–119. <https://doi.org/10.1111/j.1432-1033.1984.tb08438.x>.
40. Koo BM, Yoon MJ, Lee CR, Nam TW, Choe YJ, Jaffe H, Peterkofsky A, Seok YJ. 2004. A novel fermentation/respiration switch protein regulated by enzyme IIA^{Glc} in *Escherichia coli*. *J Biol Chem* 279:31613–31621. <https://doi.org/10.1074/jbc.M405048200>.
41. Pickering BS, Smith DR, Watnick PI. 2012. Glucose-specific enzyme IIA has unique binding partners in the *Vibrio cholerae* biofilm. *mBio* 3:e00228-12. <https://doi.org/10.1128/mBio.00228-12>.
42. Scholl D, Nixon BT. 1996. Cooperative binding of DctD to the *dctA* upstream activation sequence of *Rhizobium meliloti* is enhanced in a constitutively active truncated mutant. *J Biol Chem* 271:26435–26442. <https://doi.org/10.1074/jbc.271.42.26435>.
43. Bramley HF, Kornberg HL. 1987. Nucleotide sequence of *bglC*, the gene specifying enzyme II^{bgl} of the PEP:sugar phosphotransferase system in *Escherichia coli* K12 and overexpression of the gene product. *J Gen Microbiol* 133:563–573.
44. Iuchi S, Cole ST, Lin EC. 1990. Multiple regulatory elements for the *glpA* operon encoding anaerobic glycerol-3-phosphate dehydrogenase and the *glpD* operon encoding aerobic glycerol-3-phosphate dehydrogenase in *Escherichia coli*: further characterization of respiratory control. *J Bacteriol* 172:179–184. <https://doi.org/10.1128/jb.172.1.179-184.1990>.
45. Weisenborn DL, Wittekindt N, Larson TJ. 1992. Structure and regulation of the *glpFK* operon encoding glycerol diffusion facilitator and glycerol kinase of *Escherichia coli* K-12. *J Biol Chem* 267:6122–6131. [https://doi.org/10.1016/S0021-9258\(18\)42670-1](https://doi.org/10.1016/S0021-9258(18)42670-1).
46. de Boer M, Broekhuizen CP, Postma PW. 1986. Regulation of glycerol kinase by enzyme III^{Glc} of the phosphoenolpyruvate:carbohydrate phosphotransferase system. *J Bacteriol* 167:393–395. <https://doi.org/10.1128/jb.167.1.393-395.1986>.
47. Kotrba P, Inui M, Yukawa H. 2001. Bacterial phosphotransferase system (PTS) in carbohydrate uptake and control of carbon metabolism. *J Biosci Bioeng* 92:502–517. <https://doi.org/10.1263/jbb.92.502>.
48. Peterkofsky A, Wang G, Seok YJ. 2006. Parallel PTS systems. *Arch Biochem Biophys* 453:101–107. <https://doi.org/10.1016/j.abb.2006.01.004>.
49. Lee KJ, Jeong CS, An YJ, Lee HJ, Park SJ, Seok YJ, Kim P, Lee JH, Lee KH, Cha SS. 2011. FrsA functions as a cofactor-independent decarboxylase to control metabolic flux. *Nat Chem Biol* 7:434–436. <https://doi.org/10.1038/nchembio.589>.
50. Deutscher J, Aké FM, Derkaoui M, Zébré AC, Cao TN, Bouraoui H, Kentache T, Mokhtari A, Milohanic E, Joyet P. 2014. The bacterial phosphoenolpyruvate:carbohydrate phosphotransferase system: regulation by protein phosphorylation and phosphorylation-dependent protein-protein interactions. *Microbiol Mol Biol Rev* 78:231–256. <https://doi.org/10.1128/MMBR.00001-14>.
51. Nam TW, Jung HI, An YJ, Park YH, Lee SH, Seok YJ, Cha SS. 2008. Analyses of Mlc-IIIB^{Glc} interaction and a plausible molecular mechanism of Mlc

- inactivation by membrane sequestration. *Proc Natl Acad Sci U S A* 105: 3751–3756. <https://doi.org/10.1073/pnas.0709295105>.
52. Bouraoui H, Ventroux M, Noirot-Gros M-F, Deutscher J, Joyet P. 2013. Membrane sequestration by the EIB domain of the mannitol permease MtlA activates the *Bacillus subtilis* *mtl* operon regulator MtlR. *Mol Microbiol* 87:789–801. <https://doi.org/10.1111/mmi.12131>.
53. Nishijyo T, Haas D, Itoh Y. 2001. The CbrA-CbrB two-component regulatory system controls the utilization of multiple carbon and nitrogen sources in *Pseudomonas aeruginosa*. *Mol Microbiol* 40:917–931. <https://doi.org/10.1046/j.1365-2958.2001.02435.x>.
54. Leigh JA, Dodsworth JA. 2007. Nitrogen regulation in bacteria and archaea. *Annu Rev Microbiol* 61:349–377. <https://doi.org/10.1146/annurev.micro.61.080706.093409>.
55. Sadykov MR, Olson ME, Halouska S, Zhu Y, Fey PD, Powers R, Somerville GA. 2008. Tricarboxylic acid cycle-dependent regulation of *Staphylococcus epidermidis* polysaccharide intercellular adhesin synthesis. *J Bacteriol* 190:7621–7632. <https://doi.org/10.1128/JB.00806-08>.
56. Tian ZX, Li QS, Buck M, Kolb A, Wang YP. 2001. The CRP-cAMP complex and downregulation of the *glnAp2* promoter provides a novel regulatory linkage between carbon metabolism and nitrogen assimilation in *Escherichia coli*. *Mol Microbiol* 41:911–924. <https://doi.org/10.1046/j.1365-2958.2001.02561.x>.
57. Niehues B, Jossek R, Kramer U, Koch A, Jarling M, Schröder W, Pape H. 2003. Isolation and characterization of maltokinase (ATP:maltose 1-phosphotransferase) from *Actinoplanes missouriensis*. *Arch Microbiol* 180: 233–239. <https://doi.org/10.1007/s00203-003-0575-y>.
58. Hoischen C, Levin J, Pitaknarongphorn S, Reizer J, Saier MH, Jr. 1996. Involvement of the central loop of the lactose permease of *Escherichia coli* in its allosteric regulation by the glucose-specific enzyme IIA of the phosphoenolpyruvate-dependent phosphotransferase system. *J Bacteriol* 178:6082–6086. <https://doi.org/10.1128/jb.178.20.6082-6086.1996>.
59. Hwang SH, Im H, Choi SH. 2021. A master regulator BrpR coordinates the expression of multiple loci for robust biofilm and rugose colony development in *Vibrio vulnificus*. *Front Microbiol* 12:679854. <https://doi.org/10.3389/fmicb.2021.679854>.
60. Greenberg EP, Hastings JW, Ulitzur S. 1979. Induction of luciferase synthesis in *Beneckeia harveyi* by other marine bacteria. *Arch Microbiol* 120: 87–91. <https://doi.org/10.1007/BF00409093>.
61. Dulbecco R, Vogt M. 1954. One-step growth curve of Western equine encephalomyelitis virus on chicken embryo cells grown *in vitro* and analysis of virus yields from single cells. *J Exp Med* 99:183–199. <https://doi.org/10.1084/jem.99.2.183>.
62. O'Toole GA, Kolter R. 1998. Initiation of biofilm formation in *Pseudomonas fluorescens* WCS365 proceeds via multiple, convergent signaling pathways: a genetic analysis. *Mol Microbiol* 28:449–461. <https://doi.org/10.1046/j.1365-2958.1998.00797.x>.
63. Enos-Berlage JL, McCarter LL. 2000. Relation of capsular polysaccharide production and colonial cell organization to colony morphology in *Vibrio parahaemolyticus*. *J Bacteriol* 182:5513–5520. <https://doi.org/10.1128/JB.182.19.5513-5520.2000>.
64. Dubois M, Gilles KA, Hamilton JK, Rebers PA, Smith F. 1956. Colorimetric method for determination of sugars and related substances. *Anal Chem* 28:350–356. <https://doi.org/10.1021/ac60111a017>.
65. Jeong HS, Jeong KC, Choi HK, Park KJ, Lee KH, Rhee JH, Choi SH. 2001. Differential expression of *Vibrio vulnificus* elastase gene in a growth phase-dependent manner by two different types of promoters. *J Biol Chem* 276: 13875–13880. <https://doi.org/10.1074/jbc.M010567200>.
66. Milton DL, O'Toole R, Horstedt P, Wolf-Watz H. 1996. Flagellin A is essential for the virulence of *Vibrio anguillarum*. *J Bacteriol* 178:1310–1319. <https://doi.org/10.1128/jb.178.5.1310-1319.1996>.
67. Park KJ, Kang MJ, Kim SH, Lee HJ, Lim JK, Choi SH, Park SJ, Lee KH. 2004. Isolation and characterization of *rpoS* from a pathogenic bacterium, *Vibrio vulnificus*: role of sigma S in survival of exponential-phase cells under oxidative stress. *J Bacteriol* 186:3304–3312. <https://doi.org/10.1128/JB.186.11.3304-3312.2004>.
68. Sambrook J, Russell DW. 2001. *Molecular cloning: a laboratory manual*, 3rd ed, vol 2. Cold Spring Harbor Laboratory Press, Cold Spring Harbor, NY.
69. Miller J. 1972. *Experiments in molecular genetics*, p 352–355. Cold Spring Harbor Laboratory, Cold Spring Harbor, NY.
70. Laemmli UK. 1970. Cleavage of structural proteins during the assembly of the head of bacteriophage T4. *Nature* 227:680–685. <https://doi.org/10.1038/227680a0>.